We are IntechOpen, the world's leading publisher of Open Access books Built by scientists, for scientists

4,800
Open access books available

122,000
International authors and editors

135M
Downloads

Our authors are among the

154
Countries delivered to

TOP 1%
most cited scientists

12.2%
Contributors from top 500 universities

CLARIVATE ANALYTICS BOOK CITATION INDEX INDEXED

WEB OF SCIENCE™

Selection of our books indexed in the Book Citation Index in Web of Science™ Core Collection (BKCI)

Interested in publishing with us?
Contact book.department@intechopen.com

Numbers displayed above are based on latest data collected.
For more information visit www.intechopen.com

13

Development of On-Site Earthquake Early Warning System for Taiwan

Chu-Chieh J. Lin[1], Pei-Yang Lin[2], Tao-Ming Chang[2], Tzu-Kun Lin[2], Yuan-Tao Weng[2], Kuo-Chen Chang[2] and Keh-Chyuan Tsai[3]
[1]*SC Solutions, Inc.*
[2]*National Center for Research on Earthquake Engineering*
[3]*National Taiwan University*
[1]*USA*
[2,3]*Taiwan*

1. Introduction

Taiwan is located between Euro-Asian and Philippines tectonic plates on the Pacific Earthquake Rim; therefore, Taiwan has suffered from the threatening of moderate earthquakes for a long time. The earthquake usually caused tremendous damages to human beings and these irreversible damages include loss of human lives, public and private properties, as well as huge adverse economic impacts. It is very difficult to avoid the damages caused by earthquake due to its widely destructive power. However, if people can receive the warning for the coming of the earthquake even by only a few seconds, the damages can be reduced due to possible appropriate reaction. The earthquake early warning system (EEWS) makes it possible to issue warning alarm before the arrival of S-wave (severe shaking) and then to provide sufficient time for quick response to prevent or reduce casualty and damages.

The idea of EEWS was originated in the U.S. (Cooper, 1868) based on the principle that transmission of the electronic signal is faster than the earthquake wave, and the typical research project goes ahead mainly in the California. Up to now, there are three types Earthquake Early Warning System (EEWS). The first type is based on the earthquake locating of local seismometer network systems, the second type is based on an on-site warning of a single seismometer, and the third type is a mixed combination of the first two types. The first type EEWS is a traditional seismological method which locate earthquake, determine magnitude using local seismometer network readings then estimate strong ground motion for other sites. In 1985, the very beginning of Personal Computer (PC) era, Heaton proposed a seismic computerized alert network model which will provide short-term warning (tens of seconds) for large epicentral distance region while a major earthquake happen. In Japan, Prof. Hakuno showed an idea of the earthquake early warning at an earlier stage. Also, JR's UrEDAS (Nakamura, 1988) is famous for their practical system. However, most seismic networks in the world cannot reach such goal. During the 1994 Northridge, 1995 Kobe earthquakes, seismic center took 30 minutes to hours to locate earthquakes. In 1999 921 Chi-Chi Taiwan earthquake, the critical information was

determined within 102 seconds. Since then, this type EEWS become mature and applicable. In 2007, Japan announced to public the first EEWS system in the world that can commercially provide earthquake warning information before the large S-wave amplitude arrives. The Real-time Earthquake Information by JMA is based on the source information as a point source and therefore the accuracy of the predicted ground motion is limited especially for a large scale earthquake. However, the limitation of first type EEWS produces a large blind zone where no warning will be received before S-wave arrives. Therefore the second type EEWS (on-site) is designed for such region. The third type EEWS is a hybrid use of regional and on-site warning methods. Although there is no real practical example, this is a reasonable research direction because the limitations of the first two types EEWS is somehow complementary. The regional EEWS is accurate but slow, the on-site EEWS is fast but less accurate. In this chapter, the development of the on-site EEWS for Taiwan is introduced. As part of the total solution of seismic hazard mitigation, an on-site earthquake early warning system (EEWS) has been developed for Taiwan. It provides time-related information including the magnitude of the earthquake, the expected arrival time of strong shaking, the seismic intensity and the peak ground acceleration (PGA) of the shaking, the dominant frequency of the earthquake and the estimation of structural response.

The development of the on-site EEWS is divided into 2 stages. The 1st stage provides a basic prediction of the earthquake, and in the 2nd stage the response of the structure is estimated. In the 1st stage, the P-wave predicated PGA method and neural networks were used to model the nonlinearities caused by the interaction of different types of earthquake ground motion and the variations in the geological media of the propagation path, and learning techniques were developed for the analysis of the earthquake seismic signal. The earthquake characteristics (PGA, amplitude, arriving time and dominate frequency… etc.) were then predicted at stage I. In the 2nd stage, two different approaches are used to satisfy the different demands for the rapid estimation of structural responses. Both modules can estimate the structural response rapidly using the output of the first stage. This rapid-estimation of structural response modulus can do the estimation online in a very short time. The user can get more information about what will happened in the coming earthquake. For different type of usage, two different modules are developed. The general modulus, which only uses the common data of the structure (height, structure type, floor, address …etc), is proposed to provide a low-cost, general-application and rapid estimation of the structural responses. For the user who needs more accurate and detail estimation of structural response, such as the hi-tech facilities, hi-raised building, power plant …etc. The customized modulus (scenario-based response predictor) provides a more accurate and detailed structural response estimation. Moreover, it can connected to the automatic control system, do the adequate decision under different levels of structural responses. With this customized modulus, the economic loss will be dramatically reduced. In order to build the two rapid estimation of the structural responses modulus, a wide range of real structural response data are needed. Only with these data, both modulus can be generated and verified. In this study, the Tai-Power building is used as the target structure; the refined FEM model is build by using FEM analysis software PISA3D. The recorded data of the structural responses from the CWB are used to refine the FEM model. After that, more than 50 on-site data and 200 free-field data are used as inputs in the FEM analysis. All the simulated structural responses from the FEM are collected into the database. This database

not only can be used in the development rapid estimation of the structural responses modulus, but also can be used in the structural health monitoring studies. By utilizing the large database collected by the Central Weather Bureau (CWB), rapid and precise results can be obtained after any major earthquake. In addition, the customized modulus can also include the actuation system, which can automatically respond and reduce the economic losses due to the earthquake.

The neural network models are applied during this development of the on-site EEWS in both stages. These neural networks are used to analyse the first-arrival of the earthquake signals in as early as 3 seconds after the first ground motion is registered by the sensors at a rate of 50 samples per second. Then, the on-site EEWS instantaneously provides a profile of information consisting of the estimates of the hazard parameters at the 1st stage and the structure response at the 2nd stage. The system is trained using the seismogram data from 2371 earthquakes recorded in Taiwan. By producing accurate and informative warnings, the system has shown the potential to significantly minimize the hazards caused by the catastrophic earthquake ground motions.

2. On-site earthquake early warning system for Taiwan

The EEWS were expected to work efficiently at the sites with certain distance from the epicenter of the earthquake and also from the observation point where the earthquake motion (P-wave) is firstly observed. However, the EEWS was classified into 'on-site warning' and 'regional warning' by Kanamori (2003). Since 2007, Japan Meteorological Agency (JMA) began the general operation of the real-time earthquake information, which is composed of earthquake occurring time and hypocenter information (the magnitude and the earthquake location) and is expected to provide warning and to substantially reduce the human and physical damage for earthquakes. The EEWS by JMA could be called as 'national warning' due to the use of JMA-NIED system (nationwide earthquake observation system). One of the technical limits is applicability to the near-source earthquakes. The 'regional' EEWS was proposed and developed first by utilizing the difference of the velocity for the beginning P-wave and destructive S-wave of the earthquake as well as the epicenter locating technology. If the earthquake epicenter can be located within several seconds, more response time for the sites with certain distance from the epicenter of the earthquake can be obtained. Although the velocity of the waves depends on density and elasticity of the medium penetrated, the typical speed for the P-wave is around 5 km/sec and the speed for the S-wave is around 3 km/sec. If the area is far from the epicenter, say 100 kilometer, then we will have at most 15 seconds reaction time before the S-wave arrives if the sensor at the observation station was able to pick up the earthquake signal (P-wave) right away and locate the epicenter within 18 seconds, as shown in Eq.1.

$$100\ (\text{km}) \div 3\ (\text{km/sec}) - 18\ (\text{sec}) = 15\ (\text{sec}) \tag{1}$$

However, if the location is less than 50 kilometer from the epicenter of the earthquake, then the 'regional' (traditional) EEWS is almost useless since reaction time is less than one second. In the other words, there are so-called "blind zone", where within the 50 kilometers radius from the epicenter, existed for the 'regional' EEWS. Therefore, the "on-site" EEWS has become increasingly important for areas located in the blind zone of the "regional"

EEWS. In addition, the effort to integrate the regional warning with on-site warning to become a more robust EEWS is noticed.

The EEWS developed in Taiwan by Central Weather Bureau (CWB) is similar to the one by JMA with so-called 'regional warning' or 'national warning'. While working with the sensor array from Taiwan Strong Motion Instrumentation Program (TSMIP), the EEWS was under testing by cooperative research institutes since 2006, but the warning is only useful for the area located outside the 50 km radius from the earthquake epicenter. Therefore the 'on-site warning' is needed for a near-source earthquake and the regional system has been developed comprising 6 observation points on a circle with radius of 30km around a nuclear power plant in Lithuania to save a lead time of 4-8 seconds. These systems do not use source information but a threshold value for issuing an alarm. In addition, the effort to integrate the regional warning with on-site warning to become a more robust EEWS is noticed.

The on-site EEWS (EEWS), as part of the total solution of seismic hazard mitigation, was under development to provide a series of time related parameters such as the magnitude of the earthquake, the time until strong shaking begins, and the seismic intensity of the shaking (peak ground acceleration). Interaction of different types of earthquake ground motion and variations in the elastic property of geological media throughout the propagation path result in a highly nonlinear function. We use P-wave predicated PGA method and neural networks to model these nonlinearities and develop learning techniques for the analysis of earthquake seismic signal. This warning system is designed to analyze the first-arrival from the earthquake signals in as little as 3 seconds after first ground motion is

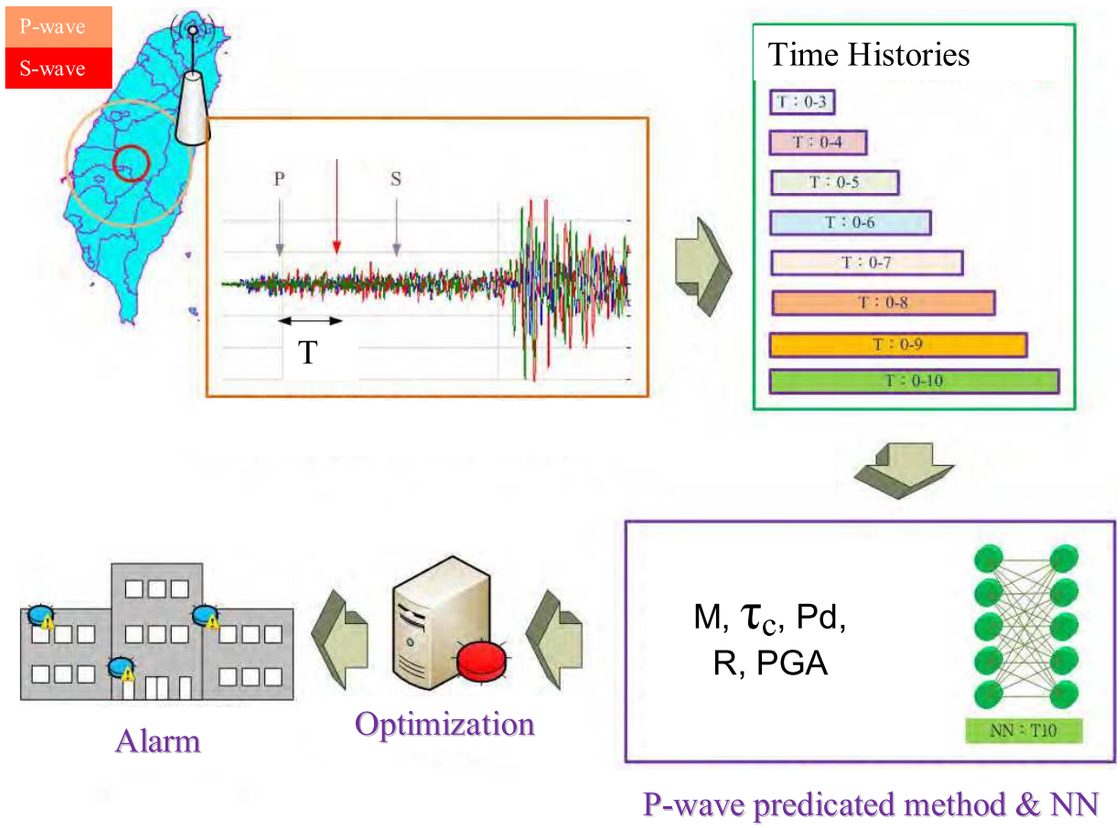

Fig. 1. The framework of the 1st stage for the on-site EEWS

felt at the sensors at a rate of 50 samples per second. Then the EEWS instantaneously provide a profile consists of the estimates of hazard parameters, such as magnitude, dominate frequency, arrival time of S-wave, and maximum seismic intensity (peak ground acceleration, PGA). The system is trained using seismogram data from more than 1000 earthquakes recorded in Taiwan. The proposed EEWS can be integrated with distributed networks for site-specific applications. By producing accurate and informative warnings, the system has the potential to significantly minimize the hazards of catastrophe ground motion. (Figure 1)

3. P-wave predicated PGA method

The major concept of the second type EEWS (on-site) is that the beginning of ground motion recorded by local seismometer can be used to predict ensuing ground motion at the same site. This is based on the physics of earthquake rupture process. Big earthquakes will have larger rupture areas and will produce longer "period" than small earthquakes if the fault rupture velocities are similar for different size earthquakes. Kanamori review the theory (hereafter τc method). The definition is

$$\tau c = \frac{1}{\sqrt{\langle f^2 \rangle}} = \frac{2\pi}{\sqrt{r}}, \quad where \quad r = \frac{\int_0^{\tau_0} \dot{u}^2(t)dt}{\int_0^{\tau_0} u^2(t)dt} = 4\pi^2 \langle f^2 \rangle \tag{2}$$

Usually τ0 is taken as 3 seconds. The ratio of first 3 second velocity ground motion with respect to displacement ground motion is related to the "period" (τc) of the initial portion of an earthquake rupture process. The log(τc) verse Mw magnitude follows a linear trend which is useful for estimating earthquake magnitude for using only one single seismometer. Wu and Kanamori applied this method to Taiwan strong motion data and provided some useful regression results.

$$M=3.088\log(\tau_c)+5.300 \tag{3}$$

$$\log(Pd)=-3.801+0.722M-1.444\log(R) \tag{4}$$

Here Pd is the maximum absolute amplitude of first 3 seconds P-wave displacement waveform, R is the epicentral distance. The attenuation relationship used in this study is provided by Dr. Jean (NCREE, Taiwan).

$$PGA=0.00284\exp(1.73306M)[R+0.09994\exp(0.77185M)]^{(-2.06392)} \tag{5}$$

The practical computation flow is described as follows.

1. Get the serial data from acceleration seismometer.
2. Compute the data stream is triggered by an earthquake or not.
3. If triggered, accumulate 3 seconds vertical component acceleration data.
4. Remove the mean and trend from data.
5. Integrate data into velocity and displacement.
6. Compute τc from integrated velocity and displacement data, then estimate earthquake magnitude.
7. Compute the maximum absolute amplitude of displacement data.
8. Estimate the epicentral distance using magnitude and amplitude information.
9. Compute the P-wave S-wave travel time difference.

10. Compute PGA from attenuation relationship by giving magnitude and distance.
11. Issue earthquake warning based on the estimated PGA

This algorithm has been used to test Taiwan strong motion acceleration data (95000 free field records). The success rate is approximate 60%. It also has been tested using building array data. The results show that the algorithm works well for seismometer installed in the basement or roof of buildings. This research result proofed that in the future application, the seismometer can be installed in any floor in a building and the prediction algorithm will not fail. Figures 2-5 show testing results using 1999 921 Chi-Chi Taiwan earthquake data recorded in the roof and basement of Taipower building which is a 26-floor with 3-floor underground structure.

Fig. 2. Photo of Taipower building.

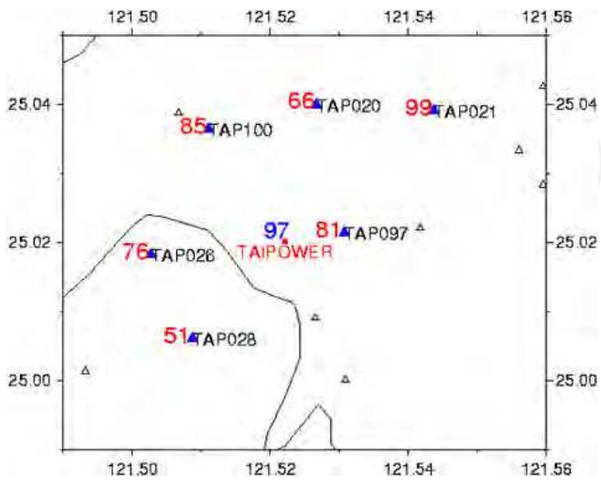

Fig. 3. The estimated ground PGA (97 gal) using Taipower building basement recorded data is reasonable comparing with the neighborhood recorded ground PGA (red number). The estimated ground PGA using roof data is 61 gal which is not shown on map.

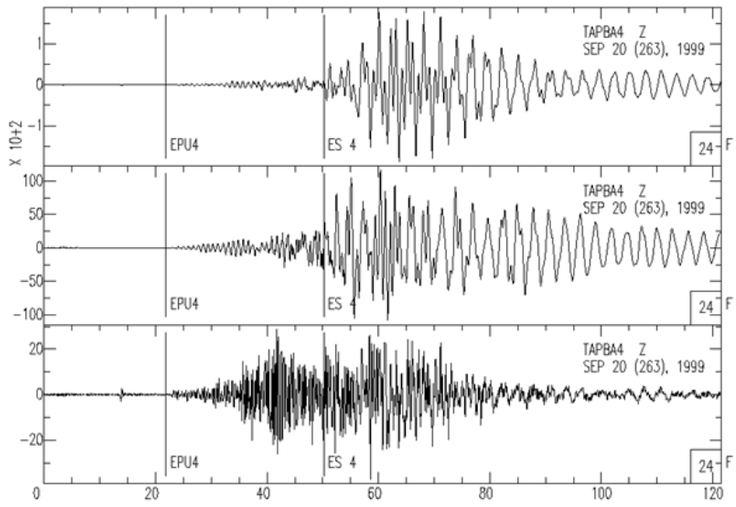

Fig. 4. The recorded 1999 921 earthquake data from the roof of Taipower building.

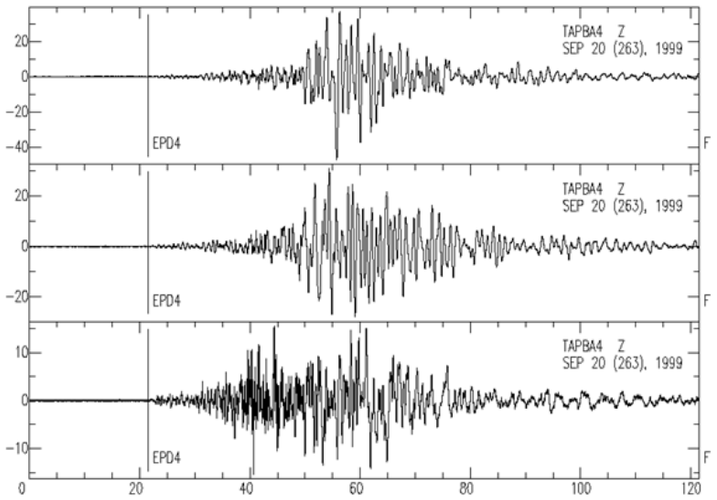

Fig. 5. The recorded 1999 921 earthquake data from the basement of Taipower building.

4. Neural network

Neural networks, that possess a massively parallel structure, are well known as a biologically inspired soft computing tool. Their learning capabilities, which differ them from other mathematically formulated methods, are provided by the unique structure of neural networks and allow the development of neural network based methods for certain mathematically intractable problems. Neural networks are formed by many interconnecting artificial neurons. Signals propagate along the connections and the strength of the transmitted signal depends on the numerical weights that are assigned to the connections. Each neuron receives signals from the incoming connections, calculates the weighted sum of the incoming signals, computes its activation function, and then sends signals along its

outgoing connections. Therefore, the knowledge learned by a neural network is stored in its connection weights. To solve difficult engineering problems, it is necessary to design a task-specific neural network. Therefore, the neural networks program developed by Lin using Fortran were used in this study. A combination of the Quick-Prop algorithm and the local adaptive learning rate algorithm were applied to the multiple-layer feed-forward (MLFF) neural networks to speed up the convergence rate of the networks. In addition, a mechanism to avoid over-training the neural networks for certain patterns, the developed algorithm was designed to monitor and equalize the influence of each pattern in the training case on the connection weights during each epoch. The average root-mean-square output error of the networks became lower while maintaining the generalization ability of the neural networks when using this adaptive process (Lin, 1999). The Neural Network has been applied to the ground motion prediction and generation since 1997. The previous researches shows that the neural network makes it possible to provide more accurate, reliable and immediate earthquake information for society by combining the national EEWS and to be applied to the advanced engineering application as well as planning of hazard mitigation (Kuyuk and Motosaka, 2009). The on-site EEWS developed for Taiwan has used initial part of P-waveform measured in-situ and neural networks for forward forecasting of ground motion parameters (Magnitude, PGA, estimated arrival time for strong motion) before S-wave arrival. The estimated ground motion information can be used as warning alarm for earthquake hazard reduction. The validity and applicability of this method have been verified by using the CWB observation data sets of 2505 earthquakes occurred in Taiwan area.

A state-of-the-art neural networks based methodology is presented for forward forecasting of ground motion parameters before S-wave arrival using initial part of P-waveform measured on-site. The estimated ground motion information can be used as warning alarm for earthquake damage reduction. The neural networks program developed by Lin using FORTRAN was used in this study. A combination of the quick-prop algorithm and the local adaptive learning rate algorithm were applied to the multiple layer feed-forward back-propagation neural networks to speed up the learning of the networks (Lin, 1999). The supercomputer is also used to train the neural networks. The validity and applicability of the method have been verified using the CWB observation data sets of 1012 earthquakes occurred in Taiwan.

Furthermore, a new concept of grouping neural networks called Expert Group Neural Network (EGNN) is also used in this study. The EGNN behaved like a group of experts, who grew up from different backgrounds with individual expertise, and were able to provide the appropriate comment when working together as a committee (Lin et al., 2006). The optimal solution among the comments will be chosen while solving this kind of problem. Eight feed forward back-propagation neural networks trained by different inputs constituted the EGNN as a committee of experts to provide the time related information from earthquake accelerograms. The architecture of each neural network among EGNN is set to be different. It consisted of one input layer with 450 to 1500 neurons, two hidden layers and one output layer with 11 neurons (as shown in Fig.6). Each of the EGNN was used to analyze the relationship between the initial few seconds of the earthquake accelerogram and the earthquake waveform information of that specific earthquake.

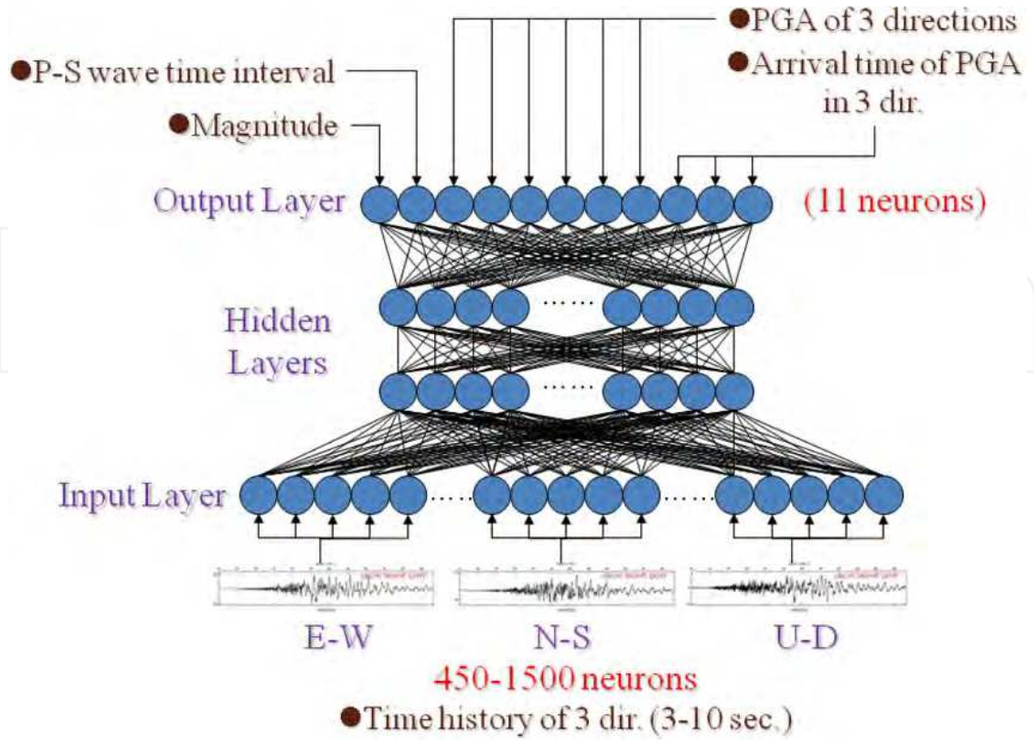

Fig. 6. The architecture of neural networks $NN_{T0\text{-}3\sim10}$

The neural networks were used in both stages of the on-site EEWS development. At the first stage development of the on-site EEWS while the parametric analysis study was conducted, the P-wave predicated PGA method (Wu and Kanamori 2005) and the neural networks were used to provide a basic prediction of the earthquake information such as the earthquake magnitude, seismic intensity, peak ground acceleration, and arrival time of S-wave for free field. In addition, the neural networks were able to predict the arrival time of PGA. The proposed method has been verified its validity and applicability. Furthermore, the neural networks were used at the 2nd stage development of the on-site EEWS to predict the seismic intensity, peak acceleration, arrival time of S-wave, and arrival time of peak acceleration for the roof of the specific building (structure response). In the first stage, the EGNN were trained with the data from first 3 seconds to 10 seconds of the earthquake accelerograms separately,. The earthquake magnitude, PGA (seismic intensity), arrival time of S-wave and arrival time of PGA were predicted using the waveform data from in-situ sensors. In this case, when the real-time information measured from the in-situ sensors is verified as earthquake using 1 second of time history after the arrival of P-wave at the site, then the initial 3 seconds of the earthquake accelerogram (P-waveform) was used as the input for the neural network (NN:T-3) to estimate the magnitude of the earthquake, the PGA (seismic intensity) in three directions, and the arrival time of the S-wave as well as those of PGA. At the same time, the sensors are recording and the initial 4, 5, .., and up to 10 seconds of P-waveform were used as the input for the neural networks (NN:T-4, NN:T-5, .., NN:T-10) to estimate the parameters for the on-site EEWS consequently. The best prediction was then chosen from these 8 results through certain optimization algorithm or time factor. The emergency response actions can be activated right after receiving the warning due to the

seismic intensity predicted for the site as well as the remaining time before the strong S-wave or PGA occurred.

The training and testing (validation) data were prepared using the earthquake accelerograms recorded through TSMIP in Taiwan from 1992 through 2006, the magnitude of these earthquake ranged from 4.0 to 8.0 on the Richter Scale. There are a total of 50149 recorded accelerograms from 2505 earthquakes. Among them, the training data were randomly chosen using 40539 earthquake records (80% of the total) from 2371 recorded earthquakes while the test data were prepared using the remaining 9610 earthquake records (20% of the total) from 1012 recorded earthquakes

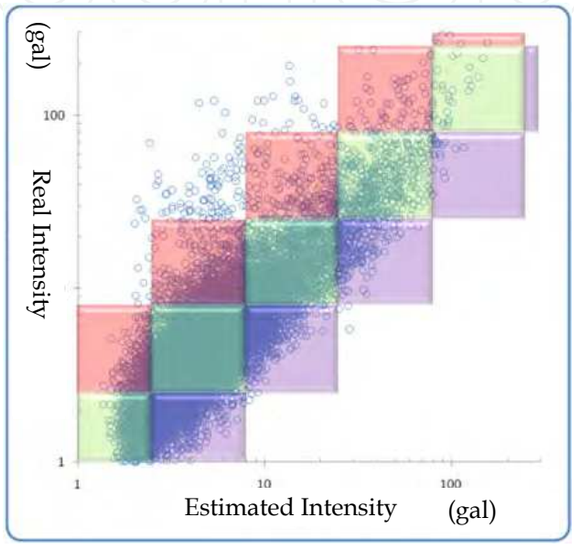

Fig. 7. Comparison of the real and est. seismic intensity ($NN_{T0\text{-}3}$)

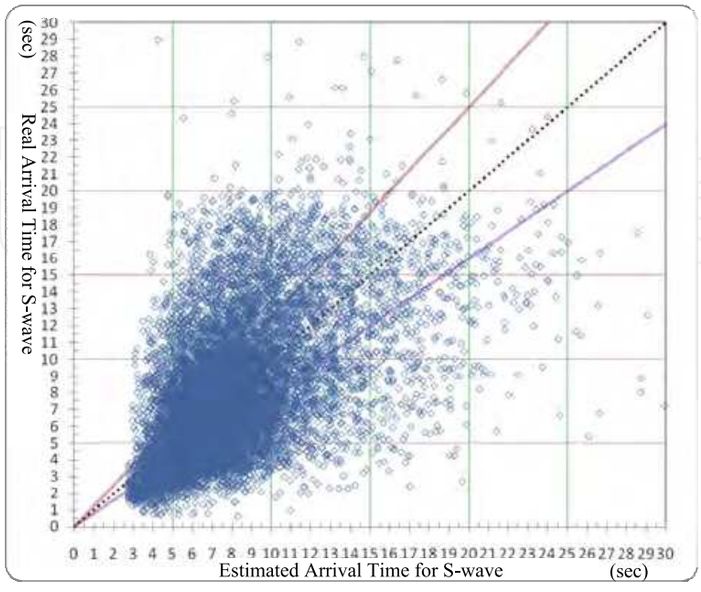

Fig. 8. Comparison of the real and est. arrival time for S-wave ($NN_{T0\text{-}3}$)

Figs. 7-8 compare the results of the prediction of seismic intensity as well as the arrival time of the S-wave for the model NN:T-3. The accuracy of the seismic intensity prediction (green area) is around 60% while the accuracy for the ± one degree seismic intensity (red, green and purple areas) is around 95% (Fig.3 R^2=0.6977). Figure 4 shows that R^2=0.28 as the accuracy for the estimated arrival time of the S-wave. If a tolerance of ±20% is considered feasible for warning people on the arrival time of S-Wave, then the accuracy is around 70%.
Figs. 9-10 compare the results of the prediction of seismic intensity as well as the arrival time of the S-wave for the model NN:T-10. The accuracy of the seismic intensity prediction (green area) is around 68% while the accuracy for the ± one degree seismic intensity (red, green and purple areas) is around 98% (Fig.3 R^2=0.7714). Figure 6 shows that R^2=0.48 as the accuracy for the estimated arrival time of the S-wave. However, the accuracy rises up to around 80% within ±20% tolerance for the purpose of warning people.

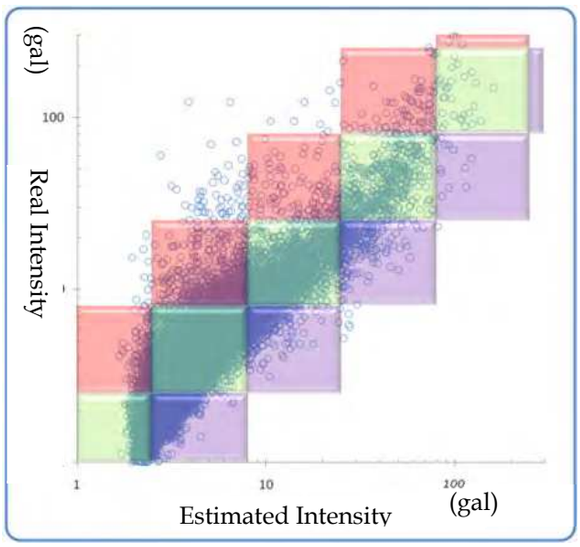

Fig. 9. Comparison of the real and est. seismic intensity ($NN_{T0\text{-}10}$)

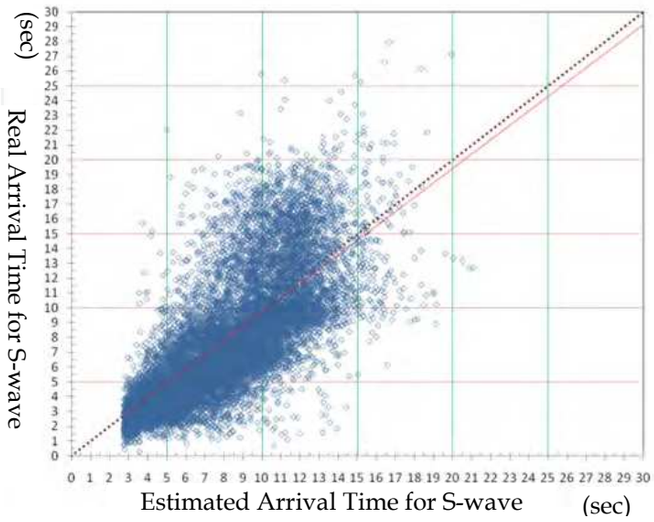

Fig. 10. Comparison of the real and est. arrival time for S-wave ($NN_{T0\text{-}10}$)

It has been found that the accuracy of the predicted peak ground motion is drastically improved compared the results of NN:T-10 to NN:T-3 since more earthquake information (7 seconds more of earthquake accelerogram) is provided for the neural network (NN:T-10), as shown in Tables 1 and 2. However, the disadvantage for model NN:T-10 is 7 seconds loss of time. Therefore, the result from NN:T-3 is recommended for the purpose of hazard mitigation and emergency response as long as the precision requirement is tolerable for certain applications. Besides, the results of the neural networks can be improved if more earthquake records can be obtained and more training can be done.

EQ	Real	T-3	T-4	T-5	T-6	T-7	T-8	T-9	T-10
A	4.75	10.00	6.77	7.41	9.36	5.84	5.79	9.24	4.59
B	10.33	9.53	9.12	5.79	14.59	8.57	8.15	5.06	11.14
C	9.29	5.85	6.44	9.93	5.98	7.84	5.78	5.29	8.98
D	5.50	7.61	8.64	2.95	6.72	6.05	7.56	8.40	5.57
E	6.79	8.85	11.07	11.36	9.98	10.35	10.38	10.08	6.58
F	11.43	8.64	14.75	10.32	12.91	7.28	8.49	6.26	11.15
G	5.07	3.29	3.51	4.31	4.37	5.13	4.13	4.68	5.47
H	9.94	7.23	9.04	7.24	4.62	5.32	3.86	3.98	9.00
I	8.99	9.19	9.40	6.52	11.09	4.94	7.71	9.49	8.43
J	9.69	10.92	11.60	9.99	13.73	9.10	7.38	11.34	11.38
K	8.18	8.19	5.16	3.74	4.38	7.02	4.60	8.33	7.42

Table 1. Comparison of the arrival time for S-wave from the neural networks with several recorded earthquakes. (Unit: second)

EQ	Real	T-3	T-4	T-5	T-6	T-7	T-8	T-9	T-10
A	2	2	3	2	2	2	3	3	2
B	3	3	3	3	3	2	3	3	3
C	2	2	2	3	3	2	2	2	2
D	4	4	4	4	3	3	4	4	4
E	2	3	3	3	2	2	2	3	2
F	3	3	3	3	4	3	3	2	4
G	3	3	4	3	3	3	3	2	3
H	5	4	4	4	4	4	4	3	5
I	4	4	4	3	4	4	4	4	4
J	3	3	3	3	3	3	3	2	3
K	3	3	3	3	3	3	3	3	3

Table 2. Comparison of the seismic intensity from the neural networks with several recorded earthquakes. (Unit: degree)

5. Rapid estimation of the structural responses / general modulus

In this section, the non-linear un-damped vibrations of an shear beam model subjected to a harmonic motion along its base are investigated. This model is applied to simulate the seismic responses of a building when peak ground acceleration (PGA) and earthquake significant frequency are predicted in part I. It is assumed that the linear part of the shear modulus of the building is uniform along the building height. Transforming the Ramberg-Osgood model to a suitable for the relationship of the shear stress versus shear strain, a non-linear partial differential equation is obtained as the governing equation. In the method presented here, the multi-story building is modelled as an equivalent continuum with non-uniform stiffness consisting of a combination of a shear cantilever beam deforming in shear configurations. The base of this building model makes as harmonic horizontal motion Asin(wt). Since the height is normalized by the total building height and nonlinear deformations occur along the transverse horizontal direction. As a result, the governing equation can be written as

$$\rho \frac{\partial \upsilon_x(z,t)}{\partial t} = \frac{\partial \tau_{xz}(z,t)}{\partial z}, \ \forall z \in (0,H), \ t \in (-\infty,+\infty) \tag{6}$$

where ρ is the mass density, υx(z,t) is the lateral velocity, z is the co-ordinate measured from the top and t is the time. Herein, the Ramberg-Osgood model is widely used as it can be transform to a suitable form for analytical solution. Rearranging this transformed model and considering the relationship between the shear stresses and strains, the non-linear stress-strain relation can be written as

$$\gamma_{xz}(z,t) = \frac{\tau_Y}{G}\{\frac{\tau_{xz}(z,t)}{\tau_Y} + \alpha[\frac{\tau_{xz}(z,t)}{\tau_Y}]^3\}, \ \forall z \in (0,H), \ t \in (-\infty,+\infty) \tag{7}$$

where τxz it the shear stress, τY it the yielding shear stress, G is the linear shear modulus and α is the post-yielding stiffness ratio. Then the equation of motion for the shear building model can be written as

$$\frac{\partial \gamma_{xz}(z,t)}{\partial t} = \frac{\partial \upsilon_{xz}(z,t)}{\partial z}, \ \forall z \in (0,H), \ t \in (-\infty,+\infty) \tag{8}$$

The shear building is subjected to a harmonic motion Asin(wt) at the base and traction free at the top. Thus, the boundary conditions can be written as

$$\tau_{xz}(0,t) = 0, \ t \in (-\infty,+\infty) \tag{9}$$

$$\upsilon_x(H,t) = \frac{\partial}{\partial t}\left[A \cdot \sin(\omega t)\right], \ t \in (-\infty,+\infty) \tag{10}$$

In this study, the response of the shear building is assumed to be harmonic with the period $2\pi/\omega$, as the forcing term. Thus the periodicity condition is written as

$$\tau_{xz}(z,t) = \tau_{xz}(z,t+2\pi/\omega), \ \forall z \in (0,H), \ t \in (-\infty,+\infty) \tag{11}$$

$$\upsilon_x(z,t) = \upsilon_x(z,t+2\pi/\omega),\ \forall z\in(0,H),\ t\in(-\infty,+\infty) \tag{12}$$

It is convenient to rewrite the above equations in terms of dimensionless quantities, which are defined as follows:

$$c=\sqrt{\frac{G}{\rho}}, \bar{z}=\frac{z}{H}, \bar{t}=\frac{ct}{H}, \gamma_Y=\frac{\tau_Y}{G}, \bar{A}=\frac{A}{\gamma_Y H}, \Omega=\frac{\omega H}{c} \tag{13}$$

where $\bar{z}$ and $\bar{t}$ are the dimensionless co-ordinate and time. $\bar{A}$ is the dimensionless displacement.
Then the system total energy E can be expressed as follows:

$$E=\int_0^1\left(\frac{1}{2}\left[\frac{\partial\hat{\phi}(z,\hat{t})}{\partial z}\right]^2+\frac{\Omega^2}{2}\left[\frac{\partial\hat{\phi}(z,\hat{t})}{\partial\hat{t}}\right]^2+\frac{3\alpha\Omega^4}{4}\left[\frac{\partial\hat{\phi}(z,\hat{t})}{\partial\hat{t}}\right]^4\right)_{t=0}dz \tag{14}$$

Due to the non-linear governing equations described above is impossible to find an exact solution. For this reason, an approximate solution is sought by using the perturbation method. Among a few variants of the perturbation method, the Lindsted-Poincaré technique seems to be a suitable one. For the use of this technique, the potential energy function $\hat{\phi}$, the system total energy E and normalized excitation frequency Ω are expanded into perturbation series in terms of ε as follows:

$$\hat{\phi}=\phi_0+\varepsilon\phi_1+\varepsilon^2\phi_2+\varepsilon^3\phi_3+..... \tag{15}$$

$$E=E_0+\varepsilon E_1+\varepsilon^2E_2+\varepsilon^3E_3+..... \tag{16}$$

$$\Omega^2=\Omega_0^2+\varepsilon\Omega_1^2+\varepsilon^2\Omega_2^2+\varepsilon^3\Omega_3^2+..... \tag{17}$$

And the system total energy can be expressed as follow:

$$\begin{aligned}E&=\int_0^1\left(\frac{1}{2}\left[\frac{\partial\hat{\phi}(z,\hat{t})}{\partial z}\right]^2+\frac{\Omega^2}{2}\left[\frac{\partial\hat{\phi}(z,\hat{t})}{\partial\hat{t}}\right]^2\right)_{t=0}dz=\frac{\Omega_0^2A^2}{2\Omega_0^2\cos^2(\Omega_0)}\int_0^1\left[\cos(\Omega_0 z)\right]^2dz\\&=\frac{\Omega_0^2A^2}{4\cos^2(\Omega_0)}\left[1+\frac{\sin(2\Omega_0)}{2\Omega_0}\right]\end{aligned} \tag{18}$$

5.1 An example

Assume that a example RC building is located in the site which seismic zone factor Z is 0.33g. The total building height H is 30 meter. The corresponding empirical period T_0 = 0.07H3/4=0.8923 sec. According the seismic force requirements of the Taiwan 1989 seismic provision, the corresponding spectral acceleration Sa(T_0) is equal to 0.33(9.8)1.2/ $\left(T_0^{2/3}\right)$ =4.1715 m/sec2. the spectral displacement SD=Sa(T_0/2π)2=0.0851 meter. If assume the ductility factor R of this building is 3.0, and the post-yielding stiffness ratio is 0.05 along the

lateral direction, then the system yielding displacement Δy= SD/R=0.0284 m. Then the perturbation factor ε can be calculated as follow:

$$\varepsilon = 0.01 \times \frac{(1-\alpha)(R-1)}{\left[1+\alpha(R-1)\right]^3} = 0.0143 \tag{19}$$

If the "P-Wave Predicted PGA Method" predicted the PGA value and the dominant frequencyω are 59.1gal and3.44 rad/sec, respectively, the peak base displacement amplitude

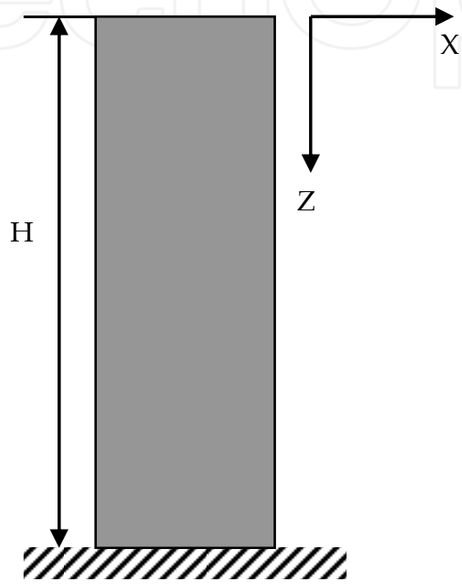

Fig. 11. Simplified shear building model

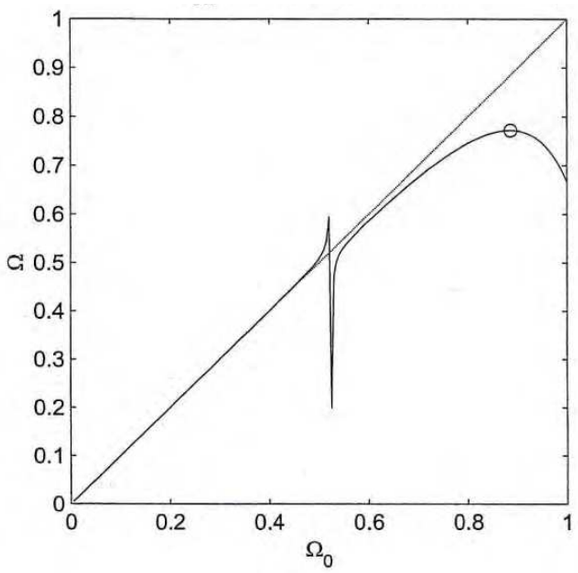

Fig. 12. The relationship between the Ω and Ω0

A is 0.05m, Substituting z=1 and A=0.05m, then the relationship between the dimensional excitation frequency Ω and the linear Ω0 can be shown as Figure2. In Figure 12, when the Ω0 is equal to the maximum value 0.885, the corresponding Ω value is 0.7715. Then the maximum story drift distribution can be shown as Figure 13. Figure 14 shows the relative displacement between the base and top of this example building.（no figure 11）

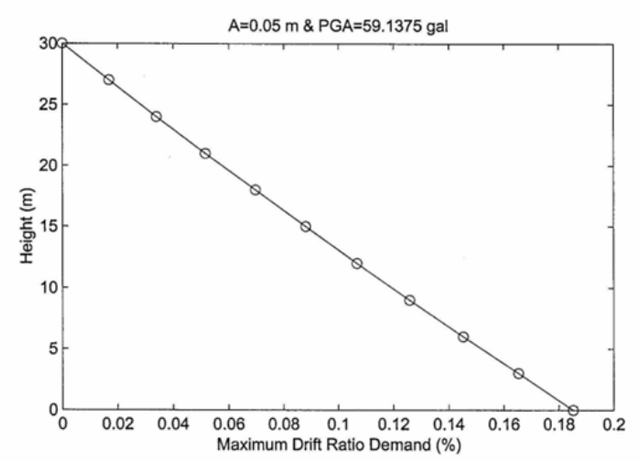

Fig. 13. The maximum drift ratio of the example building

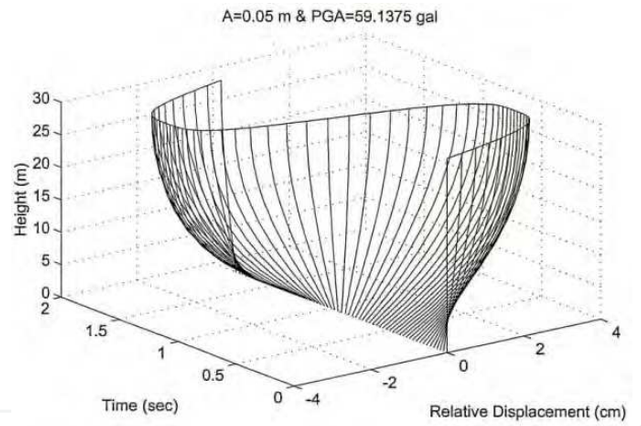

Fig. 14. The relative displacement between the base and top

6. Rapid estimation of the structural responses / customized modulus

The main target of this research is to rapidly estimate the amplification factor of structural response with the basic earthquake characteristics supported from other sub-projects. Ideally, the developed system should be able to predict the structural response accurately within 0.1 sec calculation time to protect the life and property of the whole island.

The Tai-power Building is used as the objective building in the research. By using a fine-tuned finite element model of the Tai-power Building with 60 earthquake time histories recorded in the Taipei basin, all the parameters including the PGA, earthquake magnitude, and distance between the epicenter and the local site are collected as the database for the scenario-based repression analysis.

By considering the covariance's of the amplification factors with PGA, earthquake magnitude, and epicenter, obvious relationship can be found between epicenter distance and the roof amplification factor. As the result, the epicenter distance is chosen as the governing factor to establish modules.

6.1 Regression method

The Quadratic Response Surface Model (QRSM) is used as the regression model in this scenario-based technique and the general form can be expressed as

$$y(x) = a_0 + \sum_{i=0}^{N} a_i x_i + \sum_{i<j}^{N} a_{ij} x_i x_j + \sum_{i=0}^{N} a_{ii} x_i^2 + \ldots\ldots \quad (20)$$

By choosing this model, a polynomial model with multi-variables can be easily established than the conventional nonlinear analysis process.

6.2 Analysis result

The regression results of the amplification factor on the roof floor in both X and Y directions are expressed from Figures 15 to 18.

According to the analysis result, the average error percentage of the amplification factor in the X direction is approximately 21.71% when distance between the epicenter and the site is less than 120 km, and the average error percentage in the Y direction is approximately 21.8%. Moreover, when the distance is larger than 120 km, the average error percentages reach 20% in the X direction and only 13.92% in the Y direction. In short, although some fluctuations still exist in few cases, the established regression models can generally estimate the amplification factor within several seconds after the earthquakes happen.

By using the scenario-based technique, the amplification factor of structural response can be successfully predicted by the regression models using QRSM. The theoretical analysis has demonstrated that the prediction error can be kept in an acceptable range while the result is obtained within few seconds after the major earthquakes.

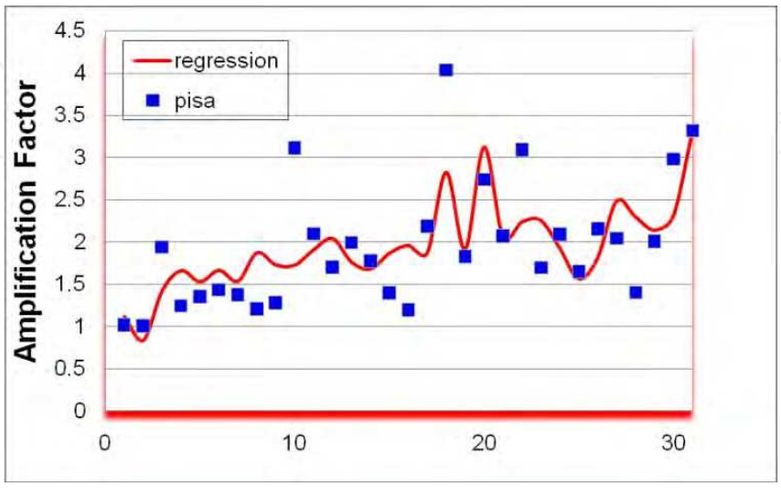

Fig. 15. Distance<120 km (X direction)

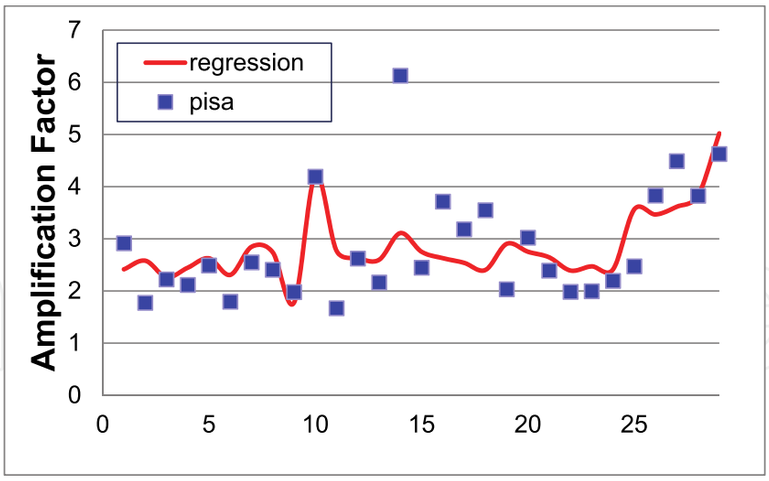

Fig. 16. Distance>120 km (X direction)

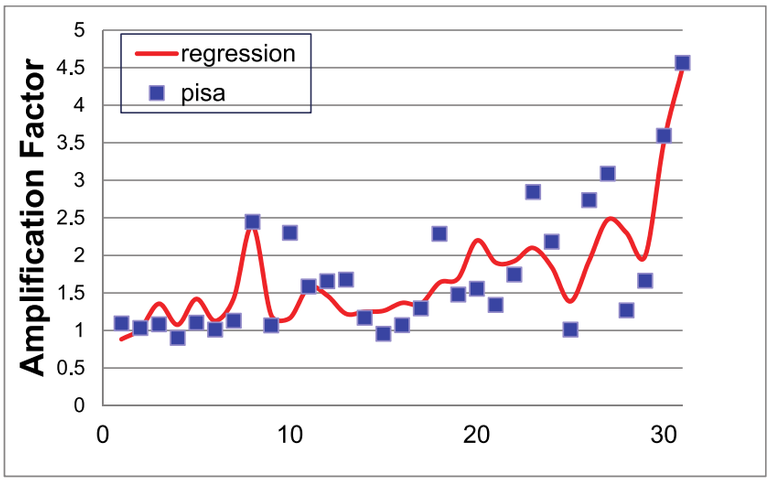

Fig. 17. Distance<120 km (Y direction)

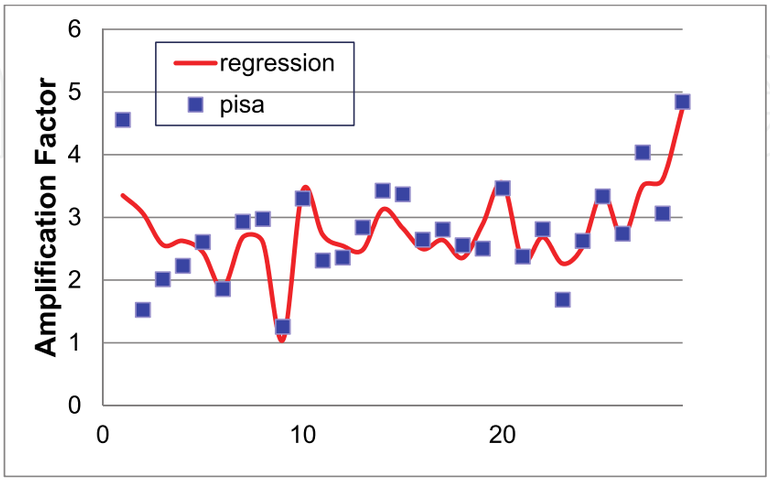

Fig. 18. Distance>120 km (Y direction)

To improve the performance of the system, the dominant frequency of the earthquake and the time difference between the P-wave and the S-wave will be considered as major factors in the regression models. Meanwhile, nonlinear model method will also be used to develop an alternative regression model. By combing these two models, it is believed that a reliable structural response prediction system can be expected in the near future.

7. Database for rapid estimated structural response

Sstructures suffered from earthquakes is concerned more and more for engineers. The earthquakes are always occurred immediately; however, how to estimate the structural response accurately and fast before the earthquake arrived is a great challenge. To achieve this end, a database contained seismic characteristics and dynamic analysis of FEM model is presented for fast estimated response of structure and the Tai-Power Building is opted as a full-scale FEM model which is constructed by using FEM analysis software PISA3D developed by NCREE.

7.1 Modification of PISA3D model

In order to estimate accurate response of structure, verification of the response between PISA3D model and reality structure should be considered. The famous Chi-Chi earthquake was chosen to compare the response of original PISA3D model and time history records of Tai-power Building. It can be seen in Figure 19 that the simulated acceleration response and

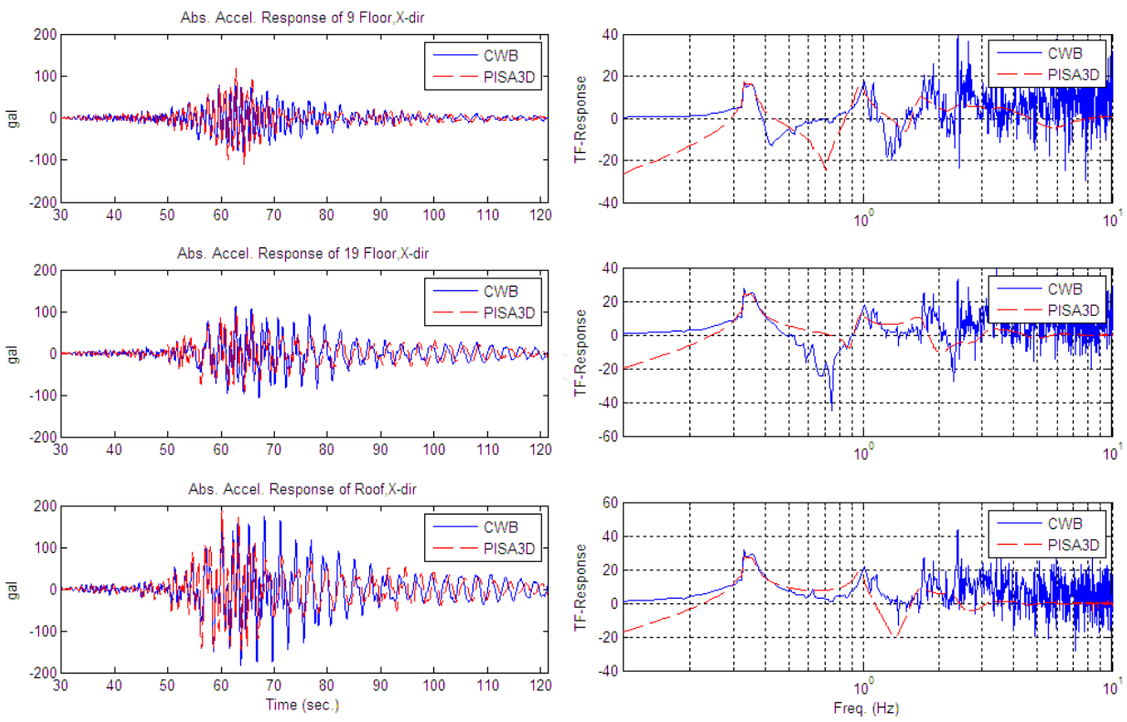

Fig. 19. Time history and transfer function of CWB records and PISA3D model in strong axis. (Excitation: Chi-Chi earthquake)

transfer function in the strong axis can be slightly regarded as consistent with the records. But as shown in Figure 20, it says that the structural response of PISA3D model in the weak axis was not estimated well as the reality structure.

From the time history and transfer function of weak axis, it figures out the structural stiffness (natural frequency) of FEM model is not sufficient as the reality structure. Therefore, modification of PISA3D model should be considered. It has several methods to modify the PISA3D model. In this case, the effect of rigid end zone and shear wall will be applied to the model to increase the stiffness of the model appropriately.

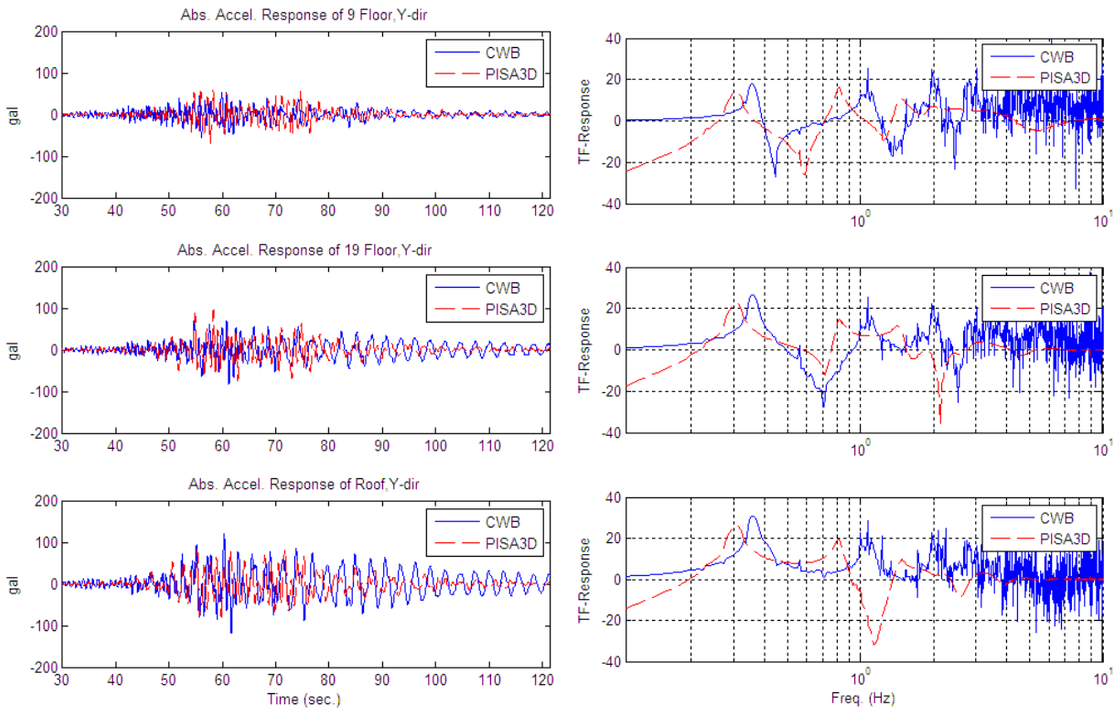

Fig. 20. Time history and transfer function of CWB records and PISA3D model in weak axis. (Excitation: Chi-Chi earthquake)

Consideration of rigid end zone and shear wall (in weak axis):

The effect of rigid end zone and shear wall shows better estimated structural response both in strong axis and weak axis. It can be shown in the Figure 21.

Besides, it's worth to mention that the dynamic characteristics of reality structure show different natural frequencies when structure suffered from different PGA of excitation. This phenomenon can be simply separated about PGA 25 gal. Two different PISA3D models, therefore, were proposed to simulate this phenomenon appropriately.

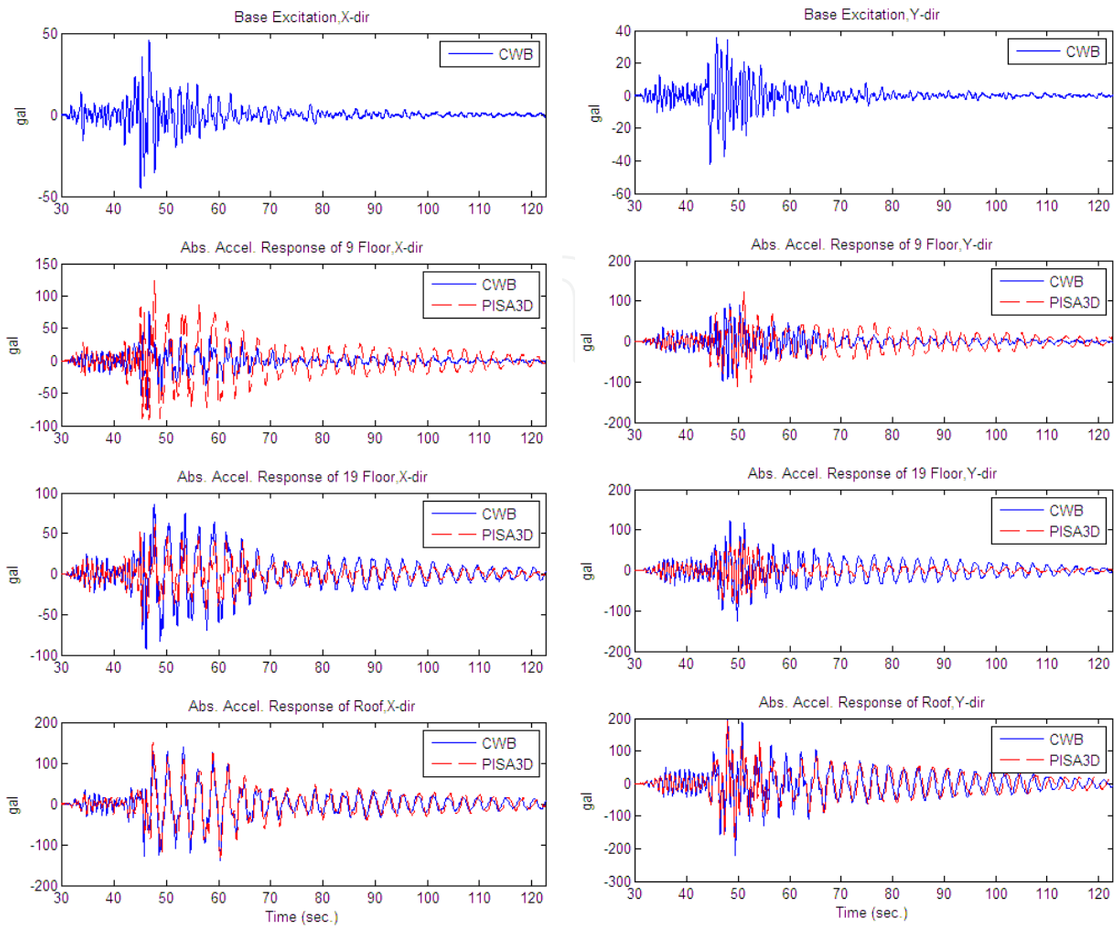

Fig. 21. Time History of CWB records and PISA3D model in strong and weak axis. (Excitation: 331 earthquake)

7.2 Construction of database

One of main purposes to construct the database is to understand structural characteristics for fast estimated response of structure suffered from different earthquakes; the other is to provide for other research such as SHM, and system identification, etc.

The contents of seismic characteristics are shown as following:

1. Coordinates of earthquake epicenter,
2. Coordinates of sensor stations,
3. Distance between epicenter and site,
4. Earthquake magnitude,
5. Site intensity,
6. Main frequency of earthquake
7. Time difference between P-wave and S-wave arrived.

And the dynamic analysis of finite element model includes:

1. Time history of structural response at specific floor
2. Time history of ground motion,
3. Peak floor acceleration
4. And PGA.

For fast estimated response of structure, the number of database should be large than a certain amount of data. However, the on-site records can not be provided as large as a database. Therefore, In Figure 22, it shows the concept to construct the database and to simulate the different site condition in Taiwan. It uses about 50 records of strong earthquake motion of Tai-power Building to verify and modify the PISA3D model, and uses more than thousands free field ground motion to excite PISA3D model to simulate the different site condition.

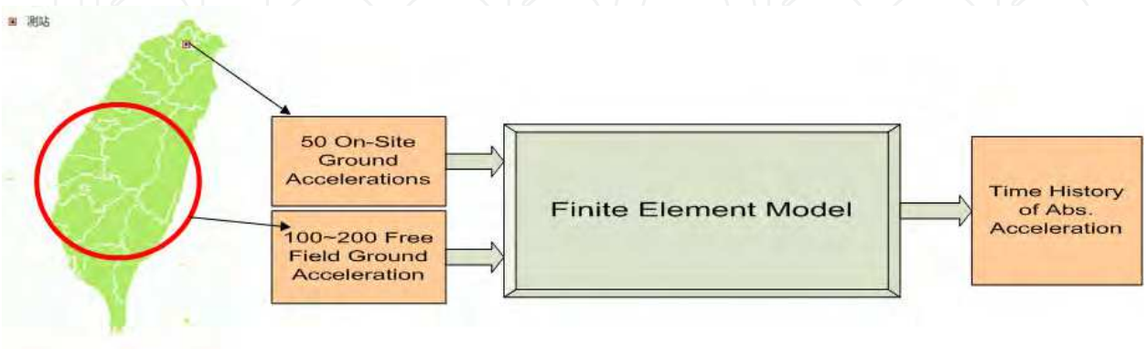

Fig. 22. Simulation of site condition in Taiwan.

7.3 Structural response prediction

This study use the recorded earthquake free field time histories collected from 1992-2006. Each earthquake record was marked P-wave and S-wave by automatically P-wave trigger program and verified manually. Then these earthquake accelerograms were consolidated into the earthquake free-field accelerogram database. Among the 59 observed buildings within the Taiwan Strong Motion Instrumentation Program (TSMIP) by CWB, the Tai-Power building is chosen since its significant features. There are totally 73 earthquake records from Tai-Power building. There are 26 time histories recorded from each sensor installed for each earthquake record. It is the tallest building when it is constructed. There are totally 26 tri-axial strong motion sensors installed in the building. Since the data recorded is not enough for training a neural network, the time history structural analysis software PISA-3D is used to build a numerical model for Tai-Power building. The 73 recorded earthquake time histories from Tai-Power building were used to modify and calibrate the numerical model of Tai-Power building. Then the chosen earthquake records from the earthquake free-field accelerogram database were used as input to run the PISA-3D and the response time histories were obtained to form the earthquake response accelerogram database. The structural response is assumed to be linear (elastic) behavior.

Usually the time history analysis for large-scale structure is time consuming because of its large linear and nonlinear analysis will affect the efficiency of calculation. Therefore, the structural analysis software PISA-3D, developed by National Center for Research on Earthquake Engineering (NCREE), is used for calculating the structural response of Tai-Power building under earthquakes due to its computational advantages for Large-scale structure and therefore the computing time required for analysis is reduced.

To increase the records of structural response for the neural network training, all the earthquake records in the earthquake free-field accelerogram database were considered and the distribution of the peak ground acceleration (PGA) were considered. The records with

PGA range from 5-500 gal were chosen to run the PISA-3D for structural response. There are totally 10,097 records were used for further analysis (Chang, K.C. et al., 2010). Figure 23 shows the flowchart of numerical building model analysis using PISA3D. All the results from PISA-3D were collected into the building response database for further research.

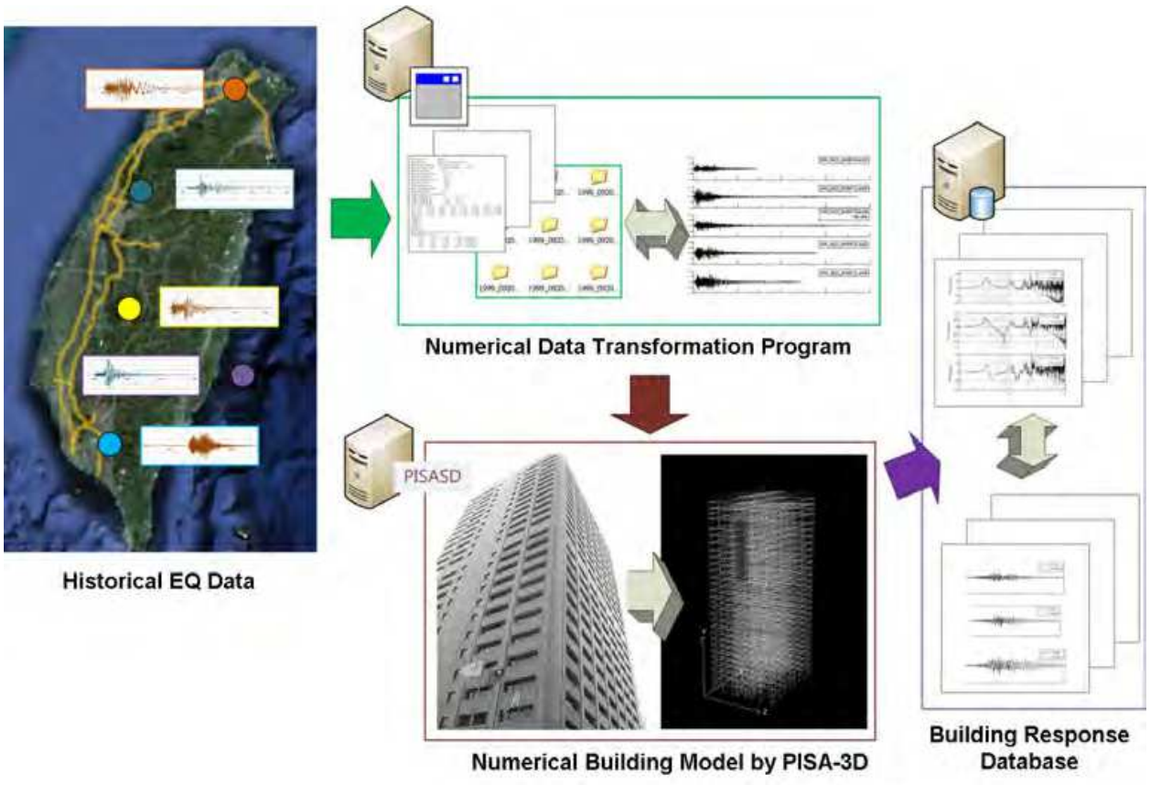

Fig. 23. Flowchart of numerical building model analysis using PISA3D

The architecture of neural networks used in this study is set to be different. Two neural networks, $NN_{T0\text{-}3}$ and $NN_{T0\text{-}10}$, were used for on-site EEWS with the Fast Fourier Transform (FFT) of the initial 3 seconds and 10 seconds sensed earthquake waveform as input respectively. Both models consisted of one input layer with 129 ($NN_{T0\text{-}3}$) or 257 ($NN_{T0\text{-}10}$) neurons, two hidden layers and one output layer with 6 neurons (as shown in Figure 24). Each of the neural networks was used to analyze the relationship between the initial three or ten seconds of the sensed earthquake accelerogram and structural response of the Tai-Power building for that specific earthquake.

In this method, the numerical model of Tai-Power building is built using PISA-3D. There are 73 earthquake records between 1994 and 2006 recorded from the sensors installed on the Tai-Power building were used to modify and calibrate the numerical model for structural response. The simulated responses for the roof of the Tai-Power building were within 10% of error. Then the 10097 earthquake records from the database of CWB were chosen as input to run the time history analysis using PISA-3D. The structural response of these 10097 earthquake records were then integrated into building response database.

The neural networks were used to learn (analyze) the relationship between free field ground motion and the structural response on the roof of the Tai-Power building. The 10097

earthquake records were divided into training group and testing group randomly. 8082 earthquake records (80% of the total) were used to train the neural networks while 2015 earthquake records (20% of the total) were used to test and validate the trained neural networks. The Fast Fourier Transform (FFT) of the digitized signal from the first 3 seconds of the earthquake time history after p-wave were used as input to the model NN_{T0-3} while the FFT from first 10 seconds of the earthquake time history were used as input to the model NN_{T0-10}. The structural responses for the roof of the Tai-Power building from the building response database were used as output for the neural networks.

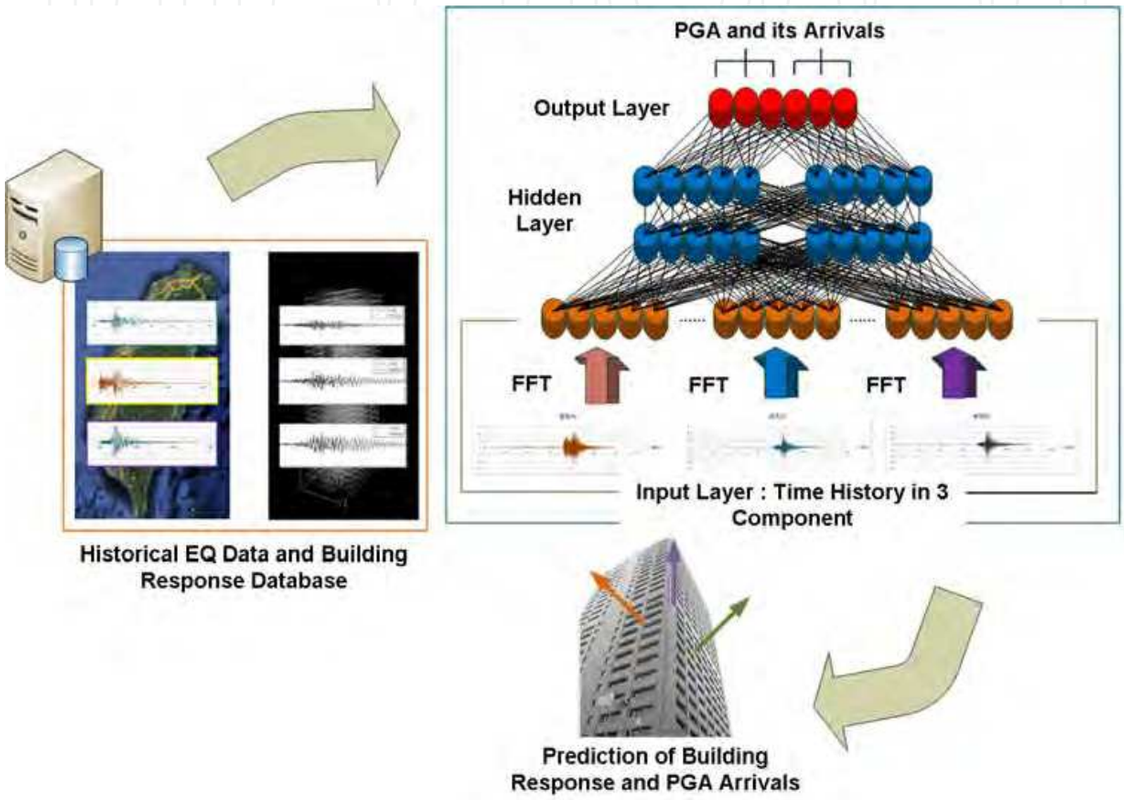

Fig. 24. Predicting structural response using neural networks

The comparison of the real and estimated seismic intensity for NN_{T0-3} and NN_{T0-10} were shown in figures 25 and 26. The results of NN estimated PGA versus the real PGA from 2015 novel testing cases is plotted in the figures. The green area means that the intensity of the NN estimated PGA is the same as the intensity of the real PGA. The red area means that the intensity of the NN estimated PGA is one grade less than the intensity of the real PGA. The purple area means that the intensity of the NN estimated PGA is one grade larger than the intensity of the real PGA. The accuracy of the intensity estimation is shown in table 3.
Both the results from NN_{T0-3} and NN_{T0-10} are acceptable and the regression analysis R^2 is 0.638 for NN_{T0-3} and 0.787 for NN_{T0-10}. It also shows better convergence in figure 4. Which shows more input information the neural network model, more accuracy result can be obtained from the neural networks. Which means NN_{T0-10} is doing better than NN_{T0-3}. If the acceptable range for the intensity prediction is set to be ±1 grade, the accuracy for NN_{T0-3} will be 91.5% (1844/2015) and 93.7% (1888/2015) for NN_{T0-10}.

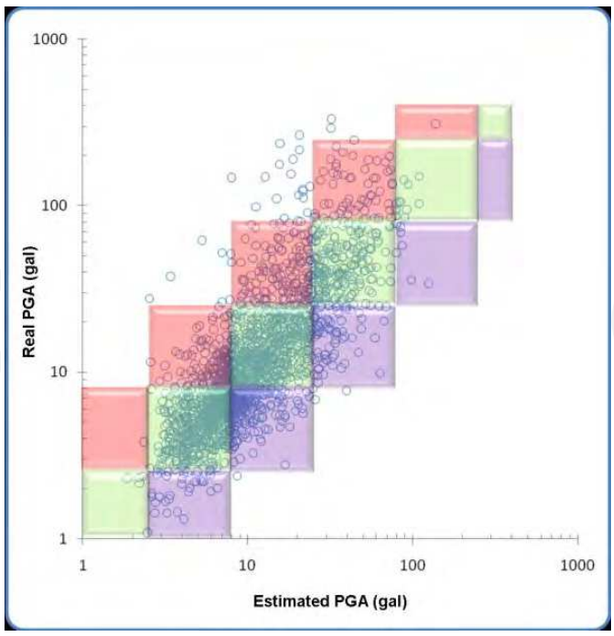

Fig. 25. Comparison of the real and est. seismic intensity (NN_{T0-3})

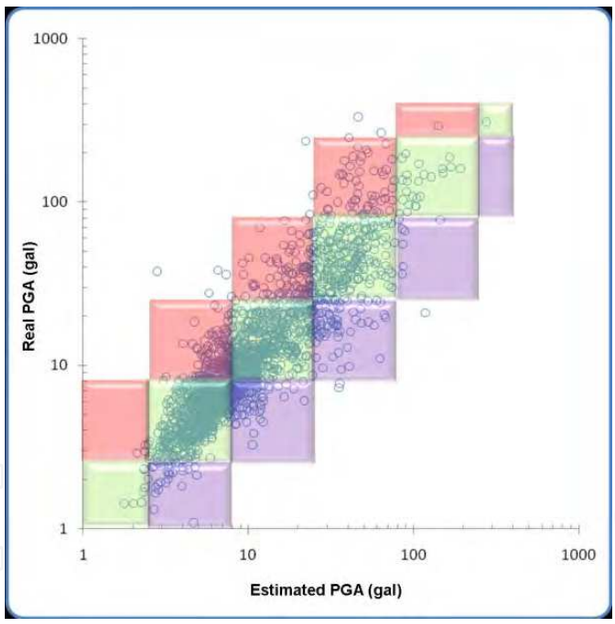

Fig. 26. Comparison of the real and est. seismic intensity (NN_{T0-10})

Error (grade) / NN model	-2	**-1**	**0**	**1**	2
NN_{T0-3}	162	**781**	**885**	**178**	2
NN_{T0-10}	120	**846**	**930**	**112**	3

Table 3. Accuracy of the intensity estimation

The comparison of the real and estimated arrival time for PGA measured on the roof in two directions (horizontal and vertical) from both NN models (NN_{T0-3} and NN_{T0-10}) were shown in figures 27-30. The results have shown convergence and the regression analysis R^2 is 0.67 for NN_{T0-3} and 0.70 for NN_{T0-10} in East-West direction. As for North-South direction, the regression analysis R^2 is 0.644 for NN_{T0-3} and 0.662 for $NN_{T0-10.}$ As for Up-Down (vertical) direction (figures 7 and 8), the regression analysis R^2 is 0.676 for NN_{T0-3} and 0.7 for $NN_{T0-10.}$ These results show that the performance of NN_{T0-10} is better than NN_{T0-3}. The conclusion can be made that more input information (longer earthquake time history) to the neural network; more accuracy of the prediction can be increased.

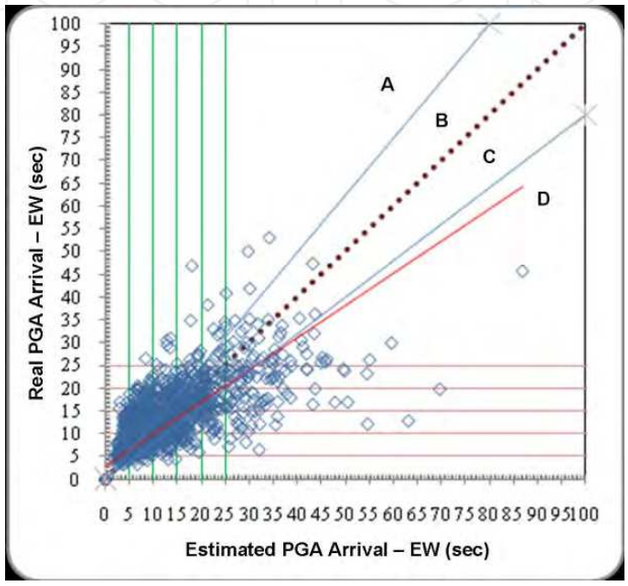

Fig. 27. Comparison of the real and est. arrival time for PGA-EW (NN_{T0-3})

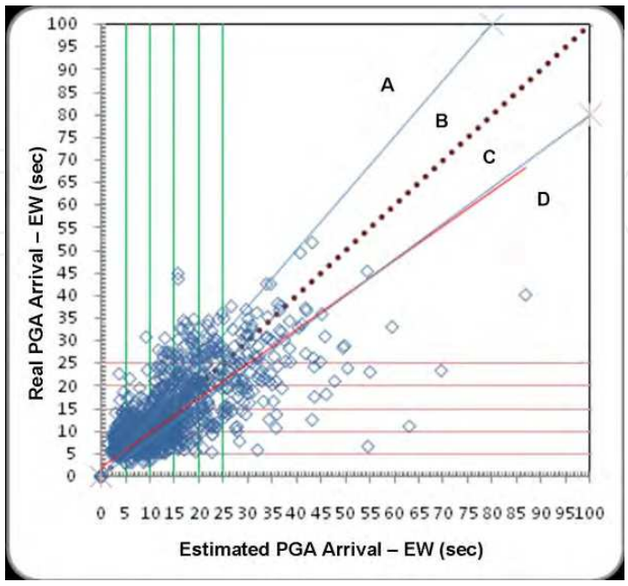

Fig. 28. Comparison of the real and est. arrival time for PGA-EW (NN_{T0-10})

In figures 27-30, the blue lines indicated the relative error of plus or minus 20% of the real values. The comparison of the real and estimated arrival time for PGA is shown in Table 4. The B area means the estimation is slightly small than the real value within 20% of error. The C area means the estimation is slightly larger than the real value within 20% of error. If the allowable error range is set to be plus or minus 20% of the real values (B and C areas indicated in figures), then the average accuracy for $NN_{T0\text{-}3}$ is 28.3% and 31.6% for $NN_{T0\text{-}10.}$ However, in the sense of early warning, the A area should be considered acceptable since the estimation is less than the real value, i.e. the warning is still effective to the people. Therefore, the allowable error range can be set to be A, B, and C areas indicated in figures, the average accuracy for $NN_{T0\text{-}3}$ is 60.2% and 66.9% for $NN_{T0\text{-}10.}$

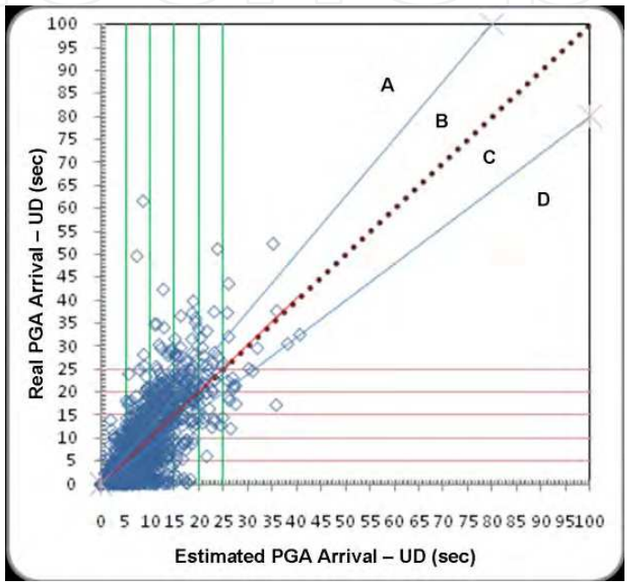

Fig. 29. Comparison of the real and est. arrival time for PGA-UD ($NN_{T0\text{-}3}$)

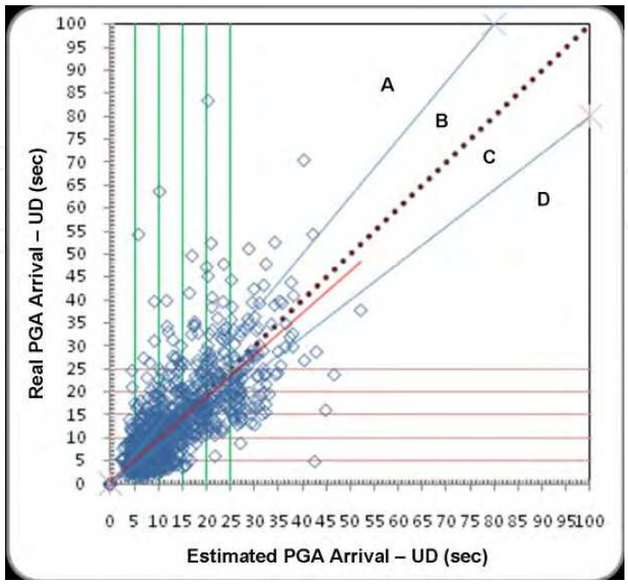

Fig. 30. Comparison of the real and est. arrival time for PGA-UD ($NN_{T0\text{-}10}$)

	NN	A	B	C	D	Total
EW	T0-3	406	289	301	1019	2015 100%
		20.15%	14.34%	14.94%	50.57%	
	T0-10	494	305	338	878	
		24.52%	15.14%	16.77%	43.57%	
NS	T0-3	1109	316	231	359	
		55.06%	15.68%	11.47%	17.83%	
	T0-10	1182	350	219	264	
		58.66%	17.37%	10.87%	13.10%	
UD	T0-3	412	263	311	1029	
		20.45%	13.05%	15.43%	51.07%	
	T0-10	460	340	356	859	
		22.83%	16.87%	17.67%	42.63%	
A: Est.< Real*80%, B: Real*80% < Est.< Real, C: Real < Est.< Real*120%, D: Real*120%< Est.						

Table 4. Comparison of the real and estimated arrival time for PGA

8. Conclusion

Preparedness is crucial when a severe earthquake occurs since most obstacles and dangers can be determined beforehand. In this chapter, the authors presented the development of the on-site EEWS on Taiwan using several different methodology including neural networks. The time issue is the key countermeasure during a large earthquake, thus a good optimization algorithm to determine immediately when and what information must be provided. Therefore, the challenge of using only 1 second of earthquake acceleration time history signal to predict earthquake information is under development. The accuracy and reliability of earthquake information is of the utmost importance and is of immense benefit in the mitigation of earthquake hazards. Furthermore, the estimation of the structural response before the arrival of the S-wave has been studied in the 2nd stage of the on-site EEWS development. The authors also presented two rapid-estimation of structural responses modulus. The general modulus, which assumed the structure as a shear beam model, can be widely applied to different type of structures. The general modulus is low-cost, widely application field and rapid estimation. In the other hand, the customized modulus can provide the more accurate and detail estimation of the structural responses. Moreover, it can connect the actuation system to dramatically reduce the economic loss due to earthquake hazard. During the development of the two rapid-estimation of structural responses modulus, the FEM analysis of the Tai-Power building is made. The real dynamic structural responses from the CWB are used to refine and verify the FEM in PISA3D. Both the on-site and free field data are used as inputs and feed into the FEM. All the simulated structural responses are collected into the database. This database can be provided to the development of the rapid-estimation of structural responses modulus. Finally, it will be

released to public for the researches of the structural health monitoring to develop and verify their algorithms.

In the future, the verification of the reliability of the communication lines as well as the system is needed to ensure reliable operation of the EEWS. Therefore, the EEWS is able to consequently bring huge benefits on the earthquake hazard mitigation. With further research on the use of the observed earthquake records, and enhancing the accuracy and immediate response of the real-time ground motion prediction, the possibility of the on-site EEWS is on the horizon.

9. Acknowledgments

We are grateful to the National Center for High-performance Computing (NCHC) for computer time and facilities used for training of the neural networks in this study.

10. References

Baer, M., and U. Kradolfer (1987). An automatic phase picker for local and teleseismic events. *Bull. Seism. Soc. Am.* 77, 1437-1445.

Chang, K.C., P.Y. Lin, C-C.J. Lin, T.K. Lin, Y.B. Lin, J.L. Lin, Y.T. Weng, T.M. Chang, S.K. Huang, Z.P. Shen, and Y.C. Lin, 2010, *Database for Fast Estimated Response of Structure*, NCREE-10-007, National Center for Research on Earthquake Engineering.

Cooper, J. D. (1868). *San Francisco Daily Evening Bulletin*, November 3.

Heaton, T. H. (1985). A model for a seismic computerized alert network, *Science* 228, 987-990.

Horiuchi, S., H. Negishi, K. Abe, A. Kamimura, and Y. Fujinawa (2005). An Automatic Processing System for Broadcasting Earthquake Alarm, *Bull. Seism. Soc. Am.* 95, 708-718.

Hsiao, N.G., 2006, *The Application of Real-Time Strong-Motion Observations on the Earthquake Early Warning in Taiwan*, PhD Thesis, Graduate Institute of Geophysics, National Central University

Kanamori, H., 2003, "On-site Earthquake Early Warning," *2nd Symposium on the real-time earthquake information transmission system*, pp.14-16.

Kanamori, H. (2005). Real-time seismology and earthquake damage mitigation, *Annu. Rev. Earth Planet. Sci.* 33, 195-214.

Kuyuk H.S., and M. Motosaka (2008). Spectral Forecasting of Earthquake Ground Motion using Regional and National EEWS for Advanced Engineering Application against Approaching Miyagi-ken Oki Earthquakes, *14th World Conference on Earthquake Engineering*, Beijing, China. S05-03-013

Kuyuk, H.S., and M. Motosaka (2009). Forward spectral forecasting of ground motion with the information of earthquake of earthquake early warning systems for structural control, *J. Japan Ass. Earthquake Engrg.* 9(3).

Lin, C-C.J. (1999). A Neural Network Based Methodology for Generating Spectrum Compatible Earthquake Accelerograms, *Ph.D. thesis, Department of Civil Engineering,* University of Illinois at Urbana-Champaign, Urbana, IL

Lin, C.-C.J., and Z.P. Shen, 2010, "Application of Neural Networks on Recent Development of the Earthquake Early Warning System for Taiwan", *Proceeding, the 9th US*

National and 10th Canadian Conference on Earthquake Engineering, (2010EQConf), Toronto, Canada.

Nakamura, Y. (1988). On the Urgent Earthquake Detection and Alarm System (UrEDAS), *Proc. 9th World Conference on Earthquake Engineering*, 673-678.

Nakamura, Y. (2005). The system development for the preparation against the unpredictable earthquake disaster, *Future Material*, 71-74. (in Japanese)

Tsai, K.C., P. Y. Lin, C-C.J. Lin, T. K. Lin, Y. B. Lin, J. L. Lin, Y. T. Weng, T. M. Chang, Z. P. Shen, and C. S. Chung, 2009, *Preliminary Study of Added-Value Information and Analysis for Earthquake Early Warning System*, NCREE-09-013, National Center for Research on Earthquake Engineering.

Wieland, M., M. Griesser, and C. Kuendig (2000). Seismic Early Warning System for a Nuclear Power Plant, *12th World Conference on Earthquake Engineering.*

Wu, Y.-M., and H. Kanamori (2005). Experiment on an onsite early warning method for the Taiwan early warning system, *Bull. Seism. Soc. Am.* 95, 347-353.

Yoshioka, K., 2006, "Outline of the Real-time Earthquake Disaster Prevention System," *Kenchiku Bosai*, pp. 22-27. (in Japanese)

Wu, Y.M. and H. Kanamori, 2005, "Experiment on an onsite early warning method for the Taiwan early warning system" *Bull. Seism. Soc. Am.*, 95, pp.347-353.

Wu, Y.M., H. Kanamori, R. Allen, and E. Hauksson, 2007, "Determination of earthquake early warning parameters, c τ and d P , for southern California," *Geophys. J. Int.*, 170, pp.711-717.

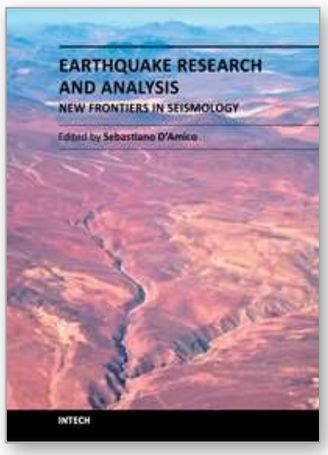

Earthquake Research and Analysis - New Frontiers in Seismology
Edited by Dr Sebastiano D'Amico

ISBN 978-953-307-840-3
Hard cover, 380 pages
Publisher InTech
Published online 27, January, 2012
Published in print edition January, 2012

The study of earthquakes combines science, technology and expertise in infrastructure and engineering in an effort to minimize human and material losses when their occurrence is inevitable. This book is devoted to various aspects of earthquake research and analysis, from theoretical advances to practical applications. Different sections are dedicated to ground motion studies and seismic site characterization, with regard to mitigation of the risk from earthquake and ensuring the safety of the buildings under earthquake loading. The ultimate goal of the book is to encourage discussions and future research to improve hazard assessments, dissemination of earthquake engineering data and, ultimately, the seismic provisions of building codes.

InTech Europe
University Campus STeP Ri
Slavka Krautzeka 83/A
51000 Rijeka, Croatia
Phone: +385 (51) 770 447
Fax: +385 (51) 686 166
www.intechopen.com

InTech China
Unit 405, Office Block, Hotel Equatorial Shanghai
No.65, Yan An Road (West), Shanghai, 200040, China
中国上海市延安西路65号上海国际贵都大饭店办公楼405单元
Phone: +86-21-62489820
Fax: +86-21-62489821

IntechOpen